Force Estimation and Slip Detection/Classification for Grip Control using a Biomimetic Tactile Sensor

Zhe Su   Karol Hausman   Yevgen Chebotar   Artem Molchanov

Gerald E. Loeb   Gaurav S. Sukhatme   Stefan Schaal

Abstract—We introduce and evaluate contact-based techniques to estimate tactile properties and detect manipulation events using a biomimetic tactile sensor. In particular, we estimate finger forces, and detect and classify slip events. In addition, we present a grip force controller that uses the estimation results to gently pick up objects of various weights and texture. The estimation techniques and the grip controller are experimentally evaluated on a robotic system consisting of Barrett arms and hands. Our results indicate that we are able to accurately estimate forces acting in all directions, detect the incipient slip, and classify slip with over 80% success rate.

I. Introduction

A service robot deployed in human environments must be able to perform dexterous manipulation tasks under many different conditions. These tasks include interacting with unknown objects (e.g. grasping). Recent advances in computer vision and range sensing enable robots to detect objects reliably [1]. However, even with a correct pose and location of an object, reliable grasping remains a problem.

Tactile sensors can be used to monitor gripper-object interactions that are very important in grasping, especially when it comes to fragile objects (see Fig. 1). These interactions are otherwise difficult to observe and model.

Achieving human level performance in dexterous grasping tasks will likely require richer tactile sensing than is currently available [2]. Recently, biomimetic tactile sensors, designed to provide more humanlike capabilities, have been developed. These new sensors provide an opportunity to significantly improve the robustness of robotic manipulation. In order to fully use the available information, new estimation techniques have to be developed. This paper presents a first step towards estimating some tactile properties and detecting manipulation events, such as slip, using biomimetic sensors.

In this work, we use the BioTac sensors [3] (Fig. 3) in order to estimate forces, detect slip events and classify the type of slip. Additionally, we present a grip controller that uses the above techniques to improve grasp quality. The key contributions of this work are: a) a force estimation technique that outperforms the state of the art, b) two different slip detection approaches that are able to detect the slip event up to $35ms$ before it is detected by an accelerometer attached to the object, c) a slip classifier that is able to classify the types of the slip with over 80% accuracy, and d) potential applications of the above techniques to robotic grasp control.

Zhe Su and Gerald E. Loeb are with the Department of Biomedical Engineering; Karol Hausman, Yevgen Chebotar, Artem Molchanov, Stefan Schaal and Gaurav S. Sukhatme are with the Department of Computer Science, University of Southern California, Los Angeles. zhesu@usc.edu
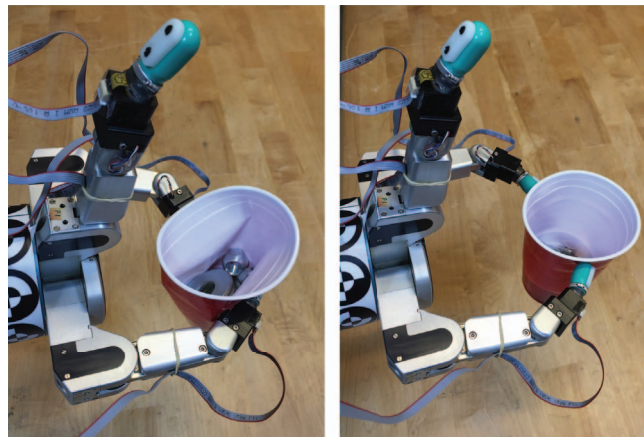
Fig. 1: Robotic arm grasping a fragile object using a standard position controller (left) and the proposed force grip controller (right).

II. Related Work

Humans are capable of manipulating novel objects with uncertain surface properties even when experiencing random external perturbations [4]. Tactile sensing plays a crucial role during these tasks [5]. As reported in [6], humans mainly rely on tactile feedback for slip detection and contact force estimation.

Previous work has taken inspiration from human grip control. Romano et al. [7] propose and evaluate a robotic grasp controller for a two-finger manipulator based on human-inspired processing of data from tactile arrays. In [8] an approach to control grip force using the BioTac is presented. The approach adopts a conservative estimate of the friction coefficient instead of estimating it on-the-fly. However, a conservative estimate may result in damaging fragile objects with excessive grip force. De Maria et al. [9] propose a new slipping avoidance algorithm based on integrated force/tactile sensors [10]. The algorithm includes a tactile exploration phase aiming to estimate the friction coefficient before grasping. It also uses a Kalman filter to track the tangential component of the force estimated from tactile sensing in order to adaptively change the grip force applied by the manipulator. In our work, instead of a tactile exploration phase, we continuously re-estimate the friction coefficient while grasping the object.

Significant work has also focused on slip detection and slip-based controllers. Heyneman and Cutkosky [11] present a method for slip detection and try to distinguish between finger/object and object/world slip events. Their approach

is based on multidimensional coherence which measures whether a group of signals is sampling a single input or a group of incoherent inputs. Schoepfer et al. [12] present a frequency-domain approach for incipient slip detection based on information from a Piezo-Resistive Tactile Sensor. Our work, however, is novel in using the BioTac sensors for these tasks, which provide the robot with increased sensitivity and frequency range over traditional sensors.

The slip classification problem has not been explored as much as the other aspects of tactile estimation. Melchiorri [13] addresses the problem of detecting both linear and rotational slip by using an integrated suite comprised of a force/torque and tactile sensors. However, this approach neglects the temporal aspect of tactile data, which may be useful in classifying manipulation events.

The BioTac sensors have been previously used to estimate contact forces. In [14] an analytical approach based on electrode impedances was used to extract normal and tangential forces. In this work, we show that our machine learning methods outperform this method substantially.

In [15] the authors also use the BioTac sensors to estimate forces acting on a finger. Machine learning (Artificial Neural Networks and Gaussian Mixture Models) are used for learning the mapping from sensor values to forces. The best performance is achieved by using neural networks with regularization techniques. Here we extend this approach to a network with multiple layers and show that it leads to better estimation performance.

III. BIOMIMETIC TACTILE SENSOR

We present a haptically-enabled robot with the Barrett arm/hand system whose three fingers are equipped with novel biomimetic tactile sensors (BioTacs). Each BioTac (see Fig. 2) consists of a rigid core housing an array of 19 electrodes surrounded by an elastic skin. The skin is inflated with an incompressible and conductive liquid.

The BioTac consists of three complementary sensory modalities: force, pressure and temperature. When the skin is in contact with an object, the liquid is displaced, resulting in distributed impedance changes in the electrode array on the surface of the rigid core. The impedance of each electrode tends to be dominated by the thickness of the liquid between the electrode and the immediately overlying skin. Slip-related micro-vibrations in the skin propagate through the fluid and are detected as AC signals by the hydro-acoustic pressure sensor. Temperature and heat flow are transduced by a thermistor near the surface of the rigid core. For each BioTac, we introduce a coordinate system that is attached to the fingernail. (Fig. 3).

IV. APPROACH

In this section, we introduce different aspects of tactile-based estimation that are useful in various manipulation scenarios. The high-resolution and multi-modal properties of the BioTac sensor enables us to estimate forces, detect and classify the slip, and control the gripper using reaction forces exerted on the fingers.
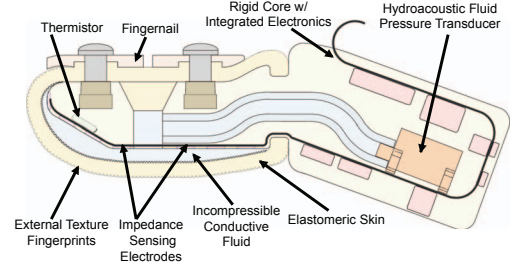

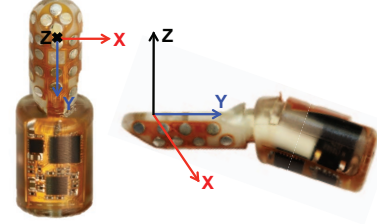Fig. 2: Cross-sectional schematic of the BioTac sensor (adapted from [14]).

Fig. 3: The coordinate frame of the BioTac sensor (adapted from [14]).

A. Force Estimation

Reliable estimation of tri-axial forces (F_x, F_y, F_z) applied on the robot finger, which are shown in Fig. 3, is important for a robust finger control. In this work, we employ and evaluate four methods to estimate these forces based on the readings from the BioTac sensor.

Previous studies have shown that tri-axial forces can be characterized based on the impedance changes on the 19 electrodes [14]. This method makes an assumption that each electrode is only sensitive to forces that are normal to its surface. In our first approach, tri-axial contact forces are analytically estimated by a weighted sum of the normal vectors $(N_{x,i}, N_{y,i}, N_{z,i})$ of the electrodes. The weights are the impedance changes (E_i) on the electrodes:

$$\begin{pmatrix} F_x \\ F_y \\ F_z \end{pmatrix} = \sum_{i=1}^{19} \begin{pmatrix} S_x E_i N_{x,i} \\ S_y E_i N_{y,i} \\ S_z E_i N_{z,i} \end{pmatrix},$$

where (S_x, S_y, S_z) are scaling factors that convert calculated contact forces into Newtons (N). They are learned with linear regression using ground truth data [14].

To improve the quality of force estimation we apply two other machine learning methods: Locally Weighted Projection Regression (LWPR) [16] and regression with neural networks. LWPR is a nonparametric regression technique that uses locally linear models to perform nonlinear function approximation. Given N local linear models $\psi_k(x)$, the estimation of the function value is performed by computing a weighted mean of the values of all local models:

$$f(\mathbf{x}) = \frac{\sum_{k=1}^{N} w_k(\mathbf{x}) \psi_k(\mathbf{x})}{\sum_{k=1}^{N} w_k(\mathbf{x})}.$$

The weights determine how much influence each local model has on the function value based on its distance from the

estimation point. The weights are commonly modelled by a Gaussian distribution:

$$w_k(\mathbf{x}) = \exp\left(-\frac{1}{2}(\mathbf{x} - \mathbf{c_k})\mathbf{D}(\mathbf{x} - \mathbf{c_k})\right),$$

where $\mathbf{c_k}$ are the centers of the Gaussians and $\mathbf{D}$ is the distance metric. Locally weighted partial least squares regression is used to learn the weights and the parameters of each local model.

As our third approach, we use a single-hidden-layer neural network (NN) that was proposed by [15] and [17]. The hidden layer consists of 38 neurons, which is the doubled number of inputs .We also propose a fourth approach, where we use a multi-layer NN to learn the mapping from BioTac electrode values to the finger forces. The network consists of input, output and three hidden layers with 10 neurons each.

For both NN approaches we use neurons with the hyperbolic tangent sigmoid transfer function:

$$a = \frac{2}{1 + \exp(-2n)} - 1.$$

For the activation of the output layer we use a linear transfer function, i.e. the output is a linear combination of the inputs from the previous layer.

NNs are trained with the error back-propagation and Levenberg-Marquardt optimization technique [18]. In order to avoid overfitting of the training data we employ the early stopping technique during training [19]. The data set is divided into mutually exclusive training, validation and test sets. While the network parameters are optimized on the training set, the training stops once the performance on the validation set starts decreasing.

B. Slip Detection

Robust slip detection is one of the most important features needed in a manipulation task. Knowledge about slip may help the robot to react such that the object does not fall out of its gripper. In order to detect a slip event, two different estimation techniques are used: a force-derivative method and a pressure-based method.

The force-derivative method uses changes in the estimated tangential force to detect slip. Because the gripper tangential force should become larger as the robot is lifting an object off a supporting surface, the negative changes of the tangential force is used to detect the slip event. Based on the experience from the experimentation, the threshold on the negative tangential force derivative is set to $-0.5N/s$.

Slip is also detected using the pressure sensor, which is digitized (12 bit resolution) in the BioTac. Since the BioTac skin contains a pattern of human-like fingerprints, it is possible to detect slip-related micro-vibration on the BioTac skin when rubbing against textured surface of an object. A bandpass filter (60-700Hz) is first employed to filter the pressure signal. Second, the resulting signal was rectified to estimate the "vibration power or slip power". Due to differences between pressure sensor sampling frequency ($2.2kHz$) and the onboard controller ($300Hz$), the slip detection algorithm considers a $10ms$ time window (3 cycles

of the onboard controller). This guarantees 22 samples of pressure readings in the time window. Slip is detected if 11 out of 22 pressure sensor values exceed the threshold. Based on the experiments, the slip threshold is set to be twice as large as the baseline vibration caused by the motors of the robot.

C. Slip Classification

In the course of our experiments we observed two main categories of object slip: linear and rotational. During linear slip, the object maintains its orientation with respect to the local end-effector frame but gradually slides out of the robot fingers. During rotational slip, the center of mass of the object tends to rotate about an axis normal to the grasp surface, although the point of contact with the robot's fingers might stay the same. It is important to discriminate between these two kinds of slip to react and control finger forces accordingly. We notice that rotational slip requires much stronger finger force response than linear slip in order to robustly keep the object grasped within the robot hand [20].

To be able to classify linear and rotational slip, we train a neural network to learn the mapping from the time-varying BioTac electrode values to the slip class. To construct the features, we take a certain time interval of electrode values and combine all values inside the window into one long feature vector, e.g. 100 consecutive timestamps of 19-dimensional electrode values result in a 1900-dimensional input vector. The architecture of the NN consists of input, output and one hidden layer with 50 neurons. The hidden layer has a sigmoid transfer function. The softmax activation function is used in the output neurons. It produces the probabilities of the signal sequence belonging to one of the slip classes.

Similar to the force estimation we use early stopping to prevent overfitting. The network is trained with the Scaled Conjugate Gradient back-propagation algorithm [21].

D. Grip Controller

In order to test the estimation of the forces and detection of the slip event, we design a grip controller that is able to take advantage of the estimated information. Appropriate grip force control is required for the robot to manipulate fragile objects without damaging or dropping them.

The control algorithm consists of two main stages, grip initiation, and object lifting (Fig. 4). In grip initiation, the robot fingers are position controlled to close on an object until the estimated normal force (F_z) is above a certain threshold. The threshold is chosen to be very small ($0.2N$) in order to avoid damaging the object. Once all the fingers are in contact with the object, the position controller is stopped, and the grip force controller is employed. The force control is used for the entire object-lifting phase.

In order to establish the minimal required grip force, the force tangential to the BioTac sensor F_t is estimated:

$$F_t = \sqrt{F_x^2 + F_y^2}.$$

Since the tangential force is directly proportional to the weight of the object, the grip force F_z is controlled based on
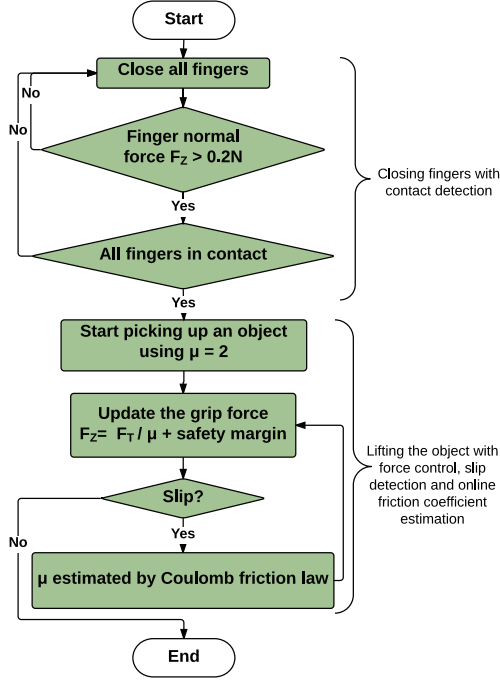
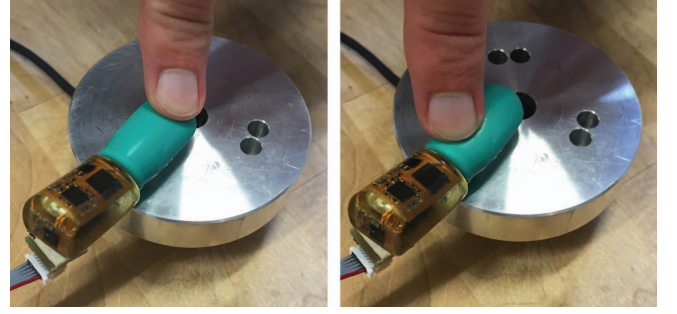Fig. 4: Control diagram of the grip controller.

Fig. 5: Experimental setup for the force estimation comparison: the finger is pressed at different positions and orientations against the force plate.
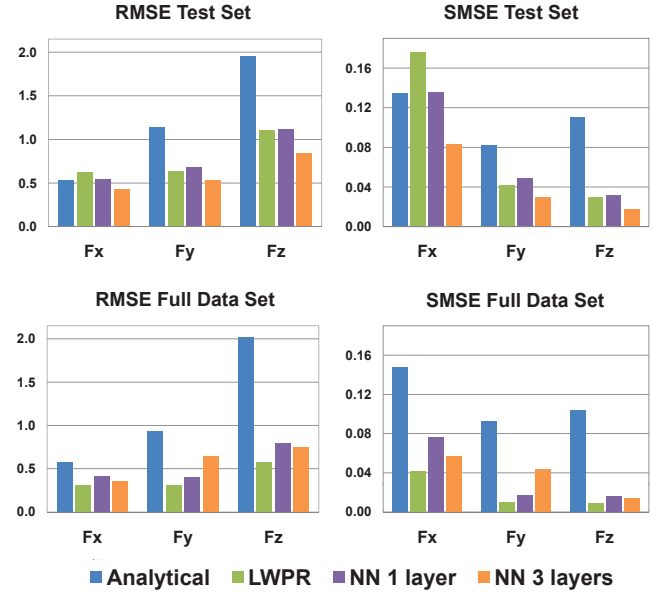

Fig. 6: The performance comparison between force estimation techniques. Analytical approach is outperformed by the other methods. LWPR and 1-layer NN perform well on the full data set but have low performance on the test set. 3-layer NN avoids overfitting and yields good results on the test set.

the current estimation of the friction coefficient μ in addition to some safety margin:

$$F_z = \frac{F_t}{\mu} + \text{safety margin}.$$

The friction coefficient is initially set to 2 based on the known friction of the silicon skin of the BioTac and other common materials. Since the initial friction coefficient is not estimated accurately, slip may occur during the lifting phase. Once slip is detected using the force-derivative-based slip detection described earlier, the friction coefficient is estimated more accurately online using the Coulomb friction law:

$$\mu = \frac{F_t}{F_z}.$$

The safety margin was chosen to be 10-40% to account for object acceleration during manipulation and additional uncertainties of the friction coefficient. Finally, the commanded grip force F_z is updated according to the newly estimated friction coefficient that provides the minimal force, which is sufficient to lift the object. The grip control algorithm is shown in Fig. 4.

V. EVALUATION AND DISCUSSION

A. Force Estimation

In order to evaluate different force estimation methods, we collected a data set consisting of raw signals of 19 electrodes. The ground truth data were acquired using a force plate that was rigidly attached to the table. The BioTac was rigidly attached to the force plate as shown in Fig. 5. In the experiment, the BioTac was perturbed manually multiple times from various directions with a wide range of forces. The data were collected with frequency 300Hz (over 17000

individual force readings). The collected data sets were divided into 30 seconds intervals of continuous electrode readings. Afterwards, these intervals were randomly shuffled and divided into 80% training and 20% test sets. Additionally, during the training of NNs, 20% of the training set was used for the validation set to prevent overfitting with the early stopping technique.

Fig. 6 shows the results of the four compared methods evaluated on the full and test sets. In both cases, common estimation metrics were chosen: Root Mean Squared Error (RMSE) of the force in N and unitless Standardized Mean Squared Error (SMSE). SMSE is computed by dividing the MSE by the variance of the data.

The analytical approach developed previously [14] is outperformed by the other three methods. From the results, we draw the conclusion that the 1-layer-NN from [17] and LWPR methods overfitted to the data, i.e. they perform better in the full dataset than the other methods but they yield
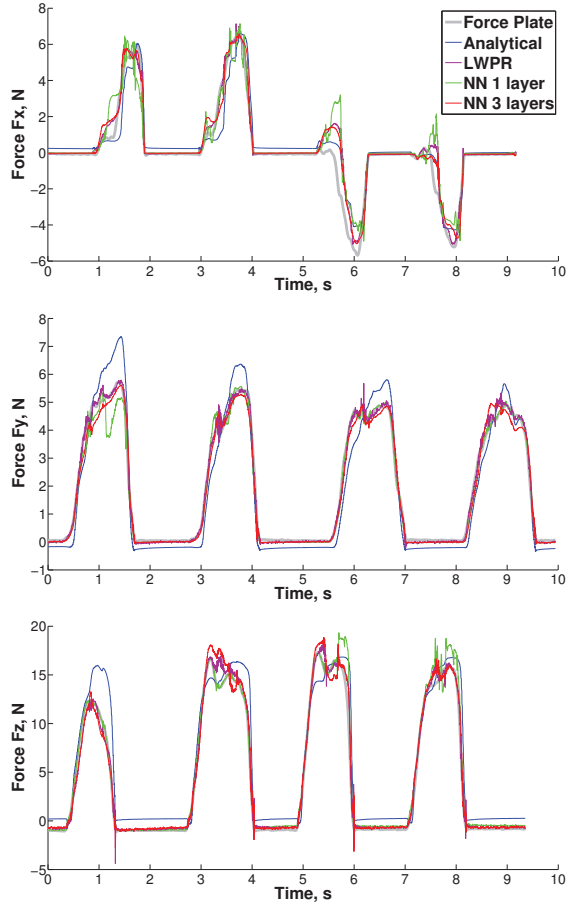
Fig. 7: Example of force estimation with different methods over time. From top to bottom: force estimation for dimensions: F_x, F_y, F_z
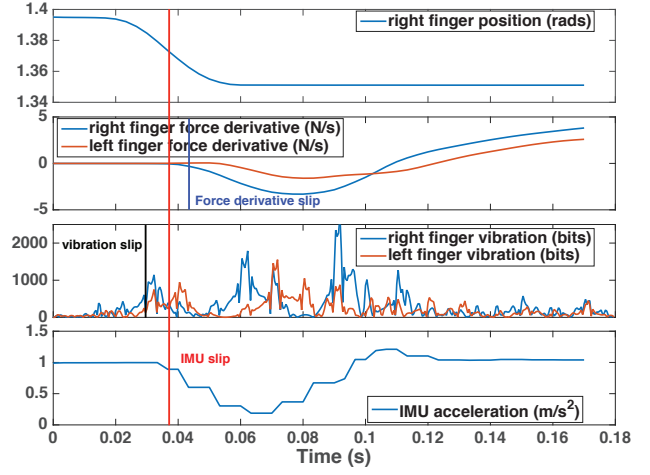

Fig. 8: An example run of the slip detection experiment. Using the BioTac sensor we are able to detect the slip event before the IMU accelerometer attached to the object measures any acceleration due to slip.

inferior performance in the set that was not exposed in the training. The 3-layer neural network approach, however, achieved good results on the test set and avoided overfitting. It illustrates that the deeper structure of the NN was able to capture the high-dimensional force mapping more accurately. On the test set, we could achieve the best RMSE of $0.43N$ in the x-direction, $0.53N$ in the y-direction and $0.85N$ in the z-direction.

It is also worth noting that there exists a significant difference between different force directions in the case of the RMSE evaluation. It can be explained by the range of forces that were exerted on the sensor. Since F_z is the vertical axis of the BioTac, the forces experienced during the experiments vary more than in the other directions. SMSE comparison is more appropriate in this case as it incorporates the range of the data. The best SMSE values on the test set were achieved with the 3-layer NN: 0.08 for the x-direction, 0.03 for the y-direction and 0.02 for the z-direction.

In addition to the absolute errors, it is important to see how the estimation errors correspond to the actual forces over time. An exemplary result is depicted in Fig. 7. One problem of the analytical approach is that it has an offset that differs in various situations. The assumption that each electrode is mostly sensitive to skin compression along its

normal vector is not able to capture the non-linear patterns given by the highly non-linear deformation on the silicon skin of the BioTac. In the case of LWPR and NNs, the results are similar. One can notice, however, that the LWPR force estimation produces forces that are not as smooth as the NN approaches. The difference between the two NN approaches is too small to be noticed on this data set. Given the results obtained from the test data set, the 3-layer NN approach yields better performance than the other methods.

B. Slip Detection

We tested the previously described slip detection algorithms on two objects with distinctive textures: a plastic jar with smooth surface and a wooden block with rough texture (see Fig. 9). In both cases, we attached an IMU to the objects in order to detect the moment when the object starts moving. In order to make the object slip, the robot first grasps and picks up the object, and then opens its right finger by 0.04 rad. The collected data set consists of 20 slip events per object.

An example run of the slip detection experiment using the wooden block is depicted in Fig. 8. One can see that using the pressure-based method, we were able to detect slip even before it was noticed by the IMU with the pressure-based method. It is also worth noting that the pressure-based method can detect slip much sooner than the force-derivative method. This may be caused by the higher sampling rate of the pressure sensor. However, it is also the case that in the very initial stage of slip (incipient slip) the microscopical slip effects are not yet visible at the electrodes. Nonetheless, the slight movement of the fingerprints is picked up by the high-frequency pressure-based slip detection signal.

Statistical analysis of the experiments shows that the robot is able to detect slip using the force-derivative method $18ms \pm 4.9ms$ (the plastic jar) and $4.7ms \pm 7.2ms$ (the wooden block) after the movement is noticed by the
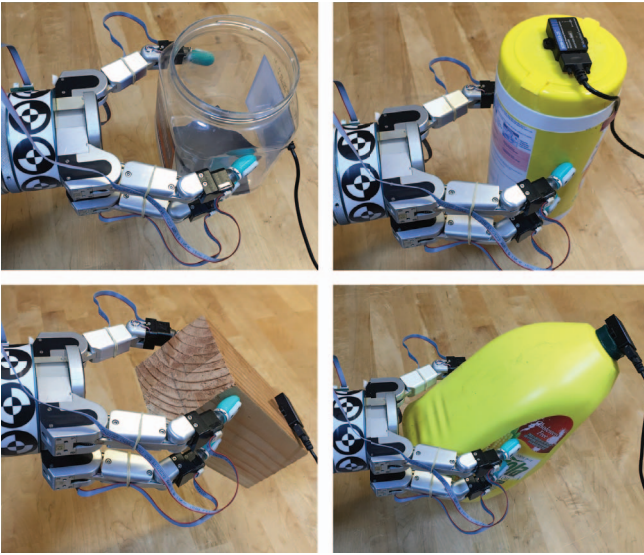
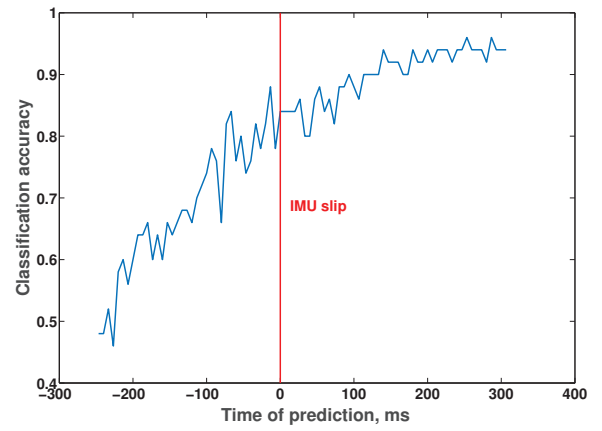Fig. 9: Different objects used for the experiments.

Fig. 10: Linear/rotational slip classification accuracy dependent on the time of prediction. Red line shows the point when slip is detected based on the IMU readings.
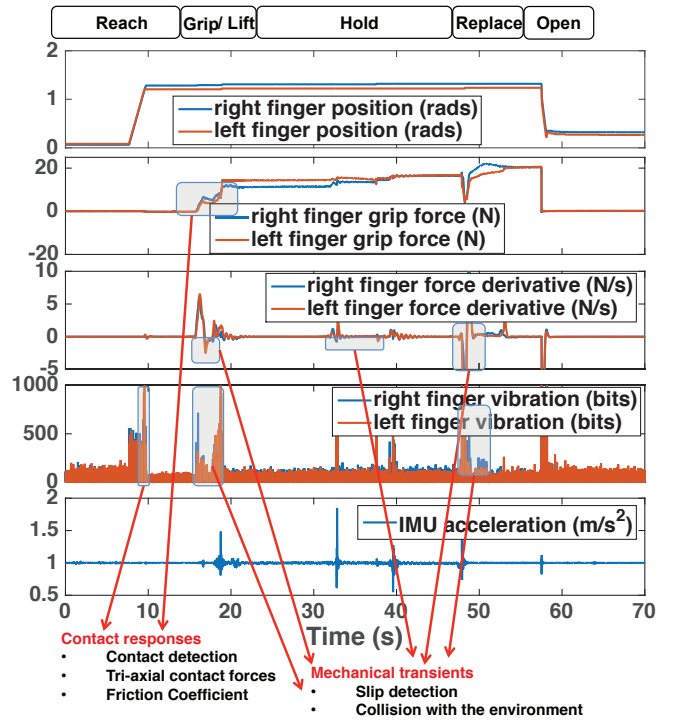
IMU. The pressure-based method detects slip even sooner: $32.8ms \pm 4.2ms$ (the plastic jar) and $35.7ms \pm 6.0ms$ (the wooden block) before the object motion is detected by the IMU. These results indicate that the BioTac is able to quickly and reliably detect slip which is important for robust grip control.

C. Slip Classification

To evaluate the NN approach for the classification of two kinds of slip events, four objects were chosen: a wooden block, oil bottle, wipes box and a jar with added weights (see Fig. 9). For training, the robot grasped an object either approximately at the center of mass of the object or at the edge of the object. These two grasping methods caused either linear (if grasped at the center of mass) or rotational slip of the object while it was being picked up. In order to detect slip, an IMU was attached to the object. For each object, over 80 grasps were performed (40 for the linear slip and 40 for the rotational slip). The data set was randomly shuffled and divided into the 80% training and 20% test sets. Similar to the force estimation, 20% of the training set was used for the validation during the NN training.

Results of the experiments are depicted in Fig. 10. For the input of the NN, points from 100 consecutive timestamps were selected, resulting in a 1900-dimensional input vector. Each point in Fig. 10 corresponds to the last timestamp that was taken into account as the NN input, i.e. the point when we classify slip given 100 previous values. The moment when slip was detected by the IMU is depicted by a vertical line. As more data are gathered during an actual slip, classification accuracy improves as expected. However, it is worth noting that using the NN approach, the robot is able to achieve approximately 80% classification rate, before the IMU is even able to notice that the slip event started. Our algorithm accurately detects the slip class even before significant object motion is detected (using an IMU), allowing more time for the robot to respond appropriately.

Fig. 11: An example run of the grip controller on the plastic jar that includes all of the grasping phases.

D. Grip Controller

The grip controller was evaluated using two different objects with varying weight: a plastic jar (see Fig. 9) with the weight ranging from $100g$ to $1500g$ and a plastic cup (see Fig. 1, top) with the weight ranging from $10g$ to $500g$. In each experiment, the robot grasped the object approximately at its center of mass, lifted it off the table, held it in the air and placed it back on the table.

Fig. 11 shows an example run of the grip controller. During the reaching phase, the robot's fingers detect the contact with the plastic jar using the normal force estimation. This is the moment when the grip force control is employed (10 seconds in the experiment). When the robot starts to

lift the jar weighted 800g, the grip force (F_z) starts to increase proportionally to the tangential force (F_t) sensed on the BioTac with 10% safety margin. The friction coefficient (μ) is updated at approximately the 18th second of the experiment, when the slip event is detected by the force-derivative method. After the 20th second of the experiment, the jar was successfully picked up and held in the air. Two 150g weight plates were added to the jar at the 32nd second and the 38th second, consecutively. It is worth noting that the grip controller detected the two slip events using the force-derivative method and increased the grip force by 2.1N and 3N to prevent further slip. When the robot placed the jar back on the table, there are large spikes in the slip detection signal (at 48th second). These may be used to detect the collision with the environment and release the objects without pressing the jar on the table with excessive force.

VI. Conclusions and Future Work

In this work, we explored how one can use biomimetic tactile sensors to extract useful tactile information needed for robust robotic grasping and manipulation.

We performed estimation of normal and tangential forces that normally occur during holding and manipulating objects. Machine learning techniques were employed and evaluated to learn the non-linear mapping from raw sensor values to forces. As the experiments demonstrated, the best performance was achieved using 3-layer neural network regression.

Different modalities available from the BioTac sensor were used to perform detection of the slip event. The best performance was observed with the pressure-based method, where slip was detected more than $30ms$ before it was picked up by an IMU accelerometer.

Slip classification into linear or rotational slip was observed to be important for robust object handling due to different requirements for finger force response. We achieved 80% classification success rate using a neural network approach before the slip event was detected by an IMU accelerometer. This indicates that the robot should be able to change finger forces at a very early stage of the slip and therefore, prevent the moving of the object inside the hand. In future work, the controller that uses this classification will be employed and evaluated.

In order to test the above mentioned estimation techniques, we created a grip force controller that adjusts the gripping force according to the forces acting on the fingers. We presented an example run of the controller during the entire grasping experiment. Our results indicate that, by using the grip controller, the robot is able to successfully grasp even easily deformable objects such as a plastic cup (Fig. 1).

At present, we are able to detect simple manipulation events and estimate forces. In the future, we plan to predict more high-level features such as grasp stability, which can be used to plan high-level decisions to manipulate objects successfully.

References

[1] D. Erhan, C. Szegedy, A. Toshev, and D. Anguelov. Scalable object detection using deep neural networks. In *Computer Vision and Pattern Recognition (CVPR), 2014 IEEE Conference on*, pages 2155–2162. IEEE, 2014.

[2] R.S. Dahiya, M. Gori, G. Metta, and G. Sandini. Better manipulation with human inspired tactile sensing. In *RSS 2009 workshop on Understanding the Human Hand for Advancing Robotic Manipulation. RSS*, pages 1–2, 2009.

[3] N. Wettels, V.J. Santos, R.S. Johansson, and G.E. Loeb. Biomimetic tactile sensor array. *Advanced Robotics*, (8):829–849, 2008.

[4] I. Birznieks, M.K.O. Burstedt, B.B. Edin, and R.S. Johansson. Mechanisms for force adjustments to unpredictable frictional changes at individual digits during two-fingered manipulation. *Journal of Neurophysiology*, 80(4):1989–2002, 1998.

[5] R.S. Johansson and R.J. Flanagan. Coding and use of tactile signals from the fingertips in object manipulation tasks. *Nature Reviews Neuroscience*, 10(5):345–359, April 2009.

[6] M.A. Srinivasan, J.M. Whitehouse, and R.H. LaMotte. Tactile detection of slip: Surface microgeometry and peripheral neural codes. *Journal of Neurophysiology*, 63:13231332, 1990.

[7] J.M. Romano, K. Hsiao, G. Niemeyer, S. Chitta, and K.J. Kuchenbecker. Human-inspired robotic grasp control with tactile sensing. *IEEE TRANSACTIONS ON ROBOTICS*, 27:1067–1079, Dec 2011.

[8] N. Wettels, A.R. Parnandi, J. Moon, G.E. Loeb, and G.S. Sukhatme. Grip control using biomimetic tactile sensing systems. *Mechatronics, IEEE/ASME Transactions on*, 14(6):718–723, 2009.

[9] G. De Maria, P. Falco, C. Natale, and S. Pirozzi. Integrated force/tactile sensing: The enabling technology for slipping detection and avoidance. In *IEEE Int. Conf. on Robotics and Automation (ICRA)*, 2015.

[10] G. De Maria, C. Natale, and S. Pirozzi. Tactile sensor for human-like manipulation. In *IEEE Int. Conf. on Biomedical Robotics and Biomechatronics*, 2012.

[11] B. Heyneman and M.R. Cutkosky. Slip interface classification through tactile signal coherence. In *IEEE Int. Conf. on Intelligent Robots and Systems (IROS)*, pages 801–808, 2013.

[12] M. Schoepfer, C. Schuermann, M. Pardowitz, and Ritter H. Using a piezo-resistive tactile sensor for detection of incipient slippage. In *IEEE Int. Symp. on Robotics*, 2010.

[13] C. Melchiorri. Slip detection and control using tactile and force sensors. *IEEE/ASME Trans. on Mechatronics*, 5(3):235242, 2000.

[14] Z. Su, J.A. Fishel, T. Yamamoto, and G.E. Loeb. Use of tactile feedback to control exploratory movements to characterize object compliance. *Frontiers in neurorobotics*, 6, 2012.

[15] N. Wettels, J.A. Fishel, and G.E. Loeb. Multimodal tactile sensor. In *The Human Hand as an Inspiration for Robot Hand Development*, volume 95 of *Springer Tracts in Advanced Robotics*, pages 405–429. Springer, 2014.

[16] S. Vijayakumar, A. D'Souza, and S. Schaal. Incremental online learning in high dimensions. *Neural Computation*, 17(12):2602–2634, 2005.

[17] N. Wettels and G.E. Loeb. Haptic feature extraction from a biomimetic tactile sensor: Force, contact location and curvature. In *ROBIO*, pages 2471–2478. IEEE, 2011.

[18] M.T. Hagan and M.B. Menhaj. Training feedforward networks with the marquardt algorithm. *Neural Networks, IEEE Transactions on*, 5(6):989–993, Nov 1994. ISSN 1045-9227.

[19] Y. Yao, L. Rosasco, and A. Caponnetto. On early stopping in gradient descent learning. *Constructive Approximation*, 26(2):289–315, 2007. ISSN 0176-4276.

[20] H. Kinoshita, L. Bäckström, J.R. Flanagan, and R.S. Johansson. Tangential torque effects on the control of grip forces when holding objects with a precision grip. *Journal of Neurophysiology*, 78(3):1619–1630, 1997.

[21] M. F. Moller. A scaled conjugate gradient algorithm for fast supervised learning. *Neural Networks*, 6(4):525–533, 1993.